

A Comprehensive Analysis on the Pion-Photon Transition Form Factor Involving the Transverse Momentum Corrections

Tao Huang^{1,2*} and Xing-Gang Wu^{3†}

¹*CCAST(World Laboratory), P.O.Box 8730, Beijing 100080, P.R.China,*

²*Institute of High Energy Physics, Chinese Academy of Sciences,
P.O.Box 918(4), Beijing 100039, P.R. China*

³*Institute of Theoretical Physics, Chinese Academy of Sciences,
P.O.Box 2735, Beijing 100080, P.R. China.*

(Dated: December 25, 2018)

Abstract

We perform a comprehensive analysis on the pion-photon transition form factor $F_{\pi\gamma}(Q^2)$ involving the transverse momentum corrections with the present CLEO experimental data. As is well-known, the valence-quark state contribution dominates of the $F_{\pi\gamma}(Q^2)$ at the large Q^2 region. One should include the contributions beyond the valence-quark state in the small Q^2 region. In this paper, we construct a phenomenological expression to estimate the contributions beyond the valence-quark state based on the asymptotic behavior of the exact prediction at $Q^2 \rightarrow 0$. Our present theoretical results agree well with the experimental data in the whole Q^2 region. Then, we extract some useful information on the pionic twist-2 distribution amplitude by comparing our results of $F_{\pi\gamma}(Q^2)$ with the CLEO data. The best fit favors the asymptotic-like behavior of the pion wavefunction.

PACS numbers: 13.40.Gp, 12.38.Bx, 12.39.Ki, 14.40.Aq

* email: huangtao@mail.ihep.ac.cn

† email: wuxg@itp.ac.cn

I. INTRODUCTION

The pion-photon transition form factor $F_{\pi\gamma}(Q^2)$, which relates two photons with one lightest meson, is the simplest example for the perturbative application to exclusive processes. It was first analyzed by Ref.[1], where the authors argued that the contributions coming from the higher Fock-states are suppressed by $1/Q^{2n}$, thus one can employ only the valence-quark state contribution to the leading order for large Q^2 region. By neglecting k_\perp (the transverse momentum of the constitute quarks) relative to q_\perp (the transverse momentum of the virtual photon) in the hard-scattering amplitude, one can obtain the leading Fock-state formula [1]:

$$F_{\pi\gamma}(Q^2) = \frac{2f_\pi}{3Q^2} \int \frac{dx}{x} \phi(x, \mu_0) \left[1 + \mathcal{O}\left(\alpha_s, \frac{m^2}{Q^2}\right) \right], \quad (1)$$

where $f_\pi = 92.4 \pm 0.25 \text{ MeV}$ [2] is the pion decay constant, $\phi(x, \mu_0)$ is the leading Fock-state distribution amplitude (DA) of pion and it is normalized as : $\int_0^1 \phi(x, \mu_0) dx = 1$. The factorization scale μ_0 is usually taken as some hadronic scale $\sim 1 \text{ GeV}$ [1, 3]. Hence, the value of $Q^2 F_{\pi\gamma}(Q^2)$ tends to be a constant ($2f_\pi$) for asymptotic DA ¹, $\phi_{as}(x) = 6x(1-x)$, as $Q^2 \rightarrow \infty$. Eq.(1) would be valid as Q^2 is large enough. However, at the end-point region $x_i \rightarrow 0, 1$ (x_i the momentum fraction of the constitute quarks in pion) and $Q^2 \sim \text{a few GeV}^2$ the wavefunction does not guarantee the k_\perp negligible. By keeping the k_\perp -corrections in both the hard-scattering amplitude and the pion wavefunction, the leading contribution to $F_{\pi\gamma}$ was given in light-cone (LC) pQCD approach by Refs.[4, 5]:

$$F_{\pi\gamma}(Q^2) = 2\sqrt{3}(e_u^2 - e_d^2) \int_0^1 [dx] \int \frac{d^2 \mathbf{k}_\perp}{16\pi^3} \Psi(x, \mathbf{k}_\perp) \times T_H(x, x', \mathbf{k}_\perp), \quad (2)$$

where $[dx] = dx dx' \delta(1 - x - x')$, $e_{u,d}$ are the quark charges in unites of e and the hard-scattering amplitude $T_H(x, x', \mathbf{k}_\perp)$ takes the form,

$$T_H(x, x', \mathbf{k}_\perp) = \frac{\mathbf{q}_\perp \cdot (x' \mathbf{q}_\perp + \mathbf{k}_\perp)}{\mathbf{q}_\perp^2 (x' \mathbf{q}_\perp + \mathbf{k}_\perp)^2} + (x \leftrightarrow x'). \quad (3)$$

The above two equations tell us that the k_\perp -corrections come from two factors: the hard-scattering amplitude $T_H(x, x', \mathbf{k}_\perp)$ and the pion wavefunction $\Psi(x, \mathbf{k}_\perp)$. With the help of Eqs.(2,3), Ref.[5] performed a careful analysis on the quark transverse-momentum effects

¹ In the following, if not specially stated, all the pion DA are in the factorization scale μ_0 and such factor will not be explicitly written for short.

to $F_{\pi\gamma}(Q^2)$. They pointed out that the transverse-momentum dependence in both the numerator and the denominator of the hard-scattering amplitude is of the same importance and should be considered consistently. Similar improved treatment has also been done in Refs.[6, 7, 8, 9, 10, 11, 12]. It was shown that pQCD can give the correct prediction for the pion-photon transition form factor that is consistent with the present experimental data after taking into account the k_\perp -dependence in both the hard-scattering amplitude and the pion wavefunction and by properly choosing of the pion wavefunction.

It should be noted that Eqs.(1,2) were obtained by assuming the valence-quark state dominance. This approximation is valid only for large Q^2 region and one can not expect these expressions can describe the present experimental data well in low Q^2 region. The approximation that the valence-quark state contribution dominant to the pion electromagnetic form factor is valid only as $Q^2 \geq 4\text{GeV}^2$, as shown in Refs.[13, 14]. A similar discussion has been done in Ref.[5] for the pion-photon transition form factor. These references tell us that one should take into account the higher Fock-state contributions as $Q^2 < a \text{ few GeV}^2$. In fact, it has been shown that the expression (2) makes a half of the contribution to $F_{\pi\gamma}(0)$ as one extends it to $Q^2 = 0$ [4]. It means that the valence-quark state contributes to $F_{\pi\gamma}(0)$ only one half and the another half is from the higher Fock-states' contributions. Both contributions from the valence and the higher Fock-states are needed to get the correct $\pi^0 \rightarrow \gamma\gamma$ rate [4]. Any attempt that involves only the valence-quark state contribution to explain both the $\pi^0 \rightarrow \gamma\gamma$ rate and the pion-photon form factor for low Q^2 region is incorrect.

In this paper, we will take the contributions from both the valence-quark state and the higher Fock-states into consideration. Especially, we will discuss how to consider the contributions beyond the valence-quark state at the low Q^2 region and give a comprehensive analysis on the pion-photon transition form factor in the whole Q^2 region. Furthermore, we can learn more information of the twist-2 DA from the present CLEO data, since the the pion-photon transition form factor in the simplest exclusive process only involving one pion and the contributions from the higher twist structure and higher helicity states are highly suppressed (at least by $1/Q^4$) in comparison to the leading-twist pion wavefunction.

The paper is organized as follows. In Sec.II, we analyze the contributions to $F_{\pi\gamma}(Q^2)$ beyond the valence-quark state at low Q^2 region under the LC pQCD approach and give a complete expression for $F_{\pi\gamma}(Q^2)$ in the whole Q^2 region. In Sec.III, we discuss what we can learn of the pionic leading-twist wavefunction/DA in comparison with CLEO experimental

data. Some further discussion and comments are made in Sec.IV. The last section is reserved for a summary.

II. AN EXPRESSION OF $F_{\pi\gamma}(Q^2)$ FROM ZERO TO LARGE Q^2 REGION

First, we give a brief review of the LC formalism [1, 15, 16]. The LC formalism provides a convenient framework for the relativistic description of hadrons in terms of quark and gluon degrees of freedom and for the application of pQCD to exclusive processes. The LC Fock-state expansion of wavefunction provides a precise definition of the parton model and a general method to calculate the hadronic matrix element. As for the pion wavefunction, its Fock state expansion is

$$|\pi\rangle = \sum |q\bar{q}\rangle \Psi_{q\bar{q}} + \sum |q\bar{q}g\rangle \Psi_{q\bar{q}g} + \dots, \quad (4)$$

where the Fock-state wavefunctions $\Psi_n(x_i, \mathbf{k}_{\perp i}, \lambda_i)$ ($n = 2, 3, \dots$) satisfy the normalization condition

$$\sum_{n, \lambda_i} \int [dx d^2 \mathbf{k}_{\perp}]_n |\Psi_n(x_i, \mathbf{k}_{\perp i}, \lambda_i)|^2 = 1, \quad (5)$$

with $[dx d^2 \mathbf{k}_{\perp}]_n = 16\pi^3 \delta(1 - \sum_{i=1}^n x_i) \delta^2(\sum_{i=1}^n \mathbf{k}_{\perp i}) \prod_{i=1}^n \left[\frac{dx_i d^2 \mathbf{k}_{\perp i}}{16\pi^3} \right]$. λ_i is the helicity of the constituents and n stands for all Fock-states, e.g. $\Psi_2 = \Psi_{q\bar{q}}$. It should be pointed out that we have $\int [dx d^2 \mathbf{k}_{\perp}]_2 \sum_{\lambda_i} |\Psi_{q\bar{q}}(x_i, \mathbf{k}_{\perp i}, \lambda_i)|^2 < 1$ for the valence-quark state.

The pion-photon transition form factor $F_{\pi\gamma}(Q^2)$ is connected with the $\pi^0 \gamma\gamma^*$ vertex in the amplitude of $e\pi \rightarrow e\gamma$ as

$$\Gamma_{\mu} = -ie^2 F_{\pi\gamma}(Q^2) \epsilon_{\mu\nu\alpha\beta} P^{\mu} \epsilon^{\alpha} q^{\beta}, \quad (6)$$

where P and q are the momenta of the incident pion and the virtual photon respectively, and ϵ is the polarization vector of the final on-shell photon. To simplify the hard-scattering amplitude, we adopt the standard momentum assignment at the ‘infinite-momentum’ frame [1], $P = (P^+, P^-, \mathbf{P}_{\perp}) = (1, 0, \mathbf{0}_{\perp})$ and $q = (0, \mathbf{q}_{\perp}^2, \mathbf{q}_{\perp})$, where P^+ is arbitrary because of Lorentz invariance and $q^2 = -\mathbf{q}_{\perp}^2 = -Q^2$. Then $F_{\pi\gamma}$ is given by

$$F_{\pi\gamma}(Q^2) = \frac{\Gamma^+}{-ie(\epsilon_{\perp} \times \mathbf{q}_{\perp})}, \quad (7)$$

where $\epsilon = (0, 0, \epsilon_{\perp})$, $\epsilon_{\perp} \cdot \mathbf{q}_{\perp} = 0$ is chosen and $\epsilon_{\perp} \times \mathbf{q}_{\perp} = \epsilon_{\perp 1} q_{\perp 2} - \epsilon_{\perp 2} q_{\perp 1}$.

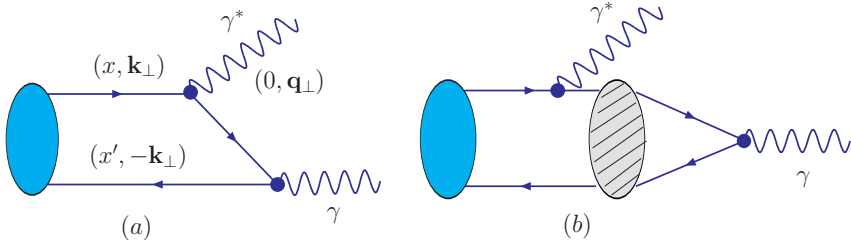


FIG. 1: Typical diagrams that contribute to $F_{\pi\gamma}(Q^2)$ form factor, where $x' = (1 - x)$. The oval with bias lines in the right diagram stands for the strong interactions.

As illustrated in Fig.(1), there are two basic types of contribution to $F_{\pi\gamma}(Q^2)$, i.e. $F_{\pi\gamma}^{(V)}(Q^2)$ and $F_{\pi\gamma}^{(NV)}(Q^2)$. $F_{\pi\gamma}^{(V)}(Q^2)$ comes from Fig.(1a), which involves the direct annihilation of $(q\bar{q})$ -pair into two photons, i.e. the valence-quark state contribution that dominates the large Q^2 contribution. $F_{\pi\gamma}^{(NV)}(Q^2)$ comes from Fig.(1b), in which one photon coupling ‘inside’ the pion wavefunction, i.e. strong interactions occur between the photon interactions that is related to the higher Fock-states’ contributions.

The first type of contribution $F_{\pi\gamma}^{(V)}(Q^2)$ (Fig.(1a)) stands for the conventional leading Fock-state contribution. Under the LC pQCD approach and by keeping the full k_T -dependence in the hard-scattering amplitude and the pion wavefunction, the expression for $F_{\pi\gamma}^{(V)}(Q^2)$ is exactly the one that is given in Eqs.(2,3). One may observe that the higher helicity states of the valence-quark state and the higher twist structures of the pion wavefunction are suppressed by $1/Q^4$ or higher, as has been discussed in Ref.[9].

As for the second type of contribution $F_{\pi\gamma}^{(NV)}(Q^2)$ (Fig.(1b)), it is difficult to be calculated in any Q^2 region. However one can calculate it in $Q^2 \sim 0$ region as suggested in Ref.[4]. Under such region, since the wavelength of the photon ‘inside’ the pion wavefunction $\sim 1/m_\pi$ is assumed to be much larger than the pion radius $1/\lambda$ (λ is some typical hadronic scale $\sim 1\text{GeV}$), we can treat such photon (nearly on-shell) as an external field which is approximately constant throughout the pion’s volume. And then, the lowest $q\bar{q}$ -wavefunction for the pion is modified only by a phase $e^{-iy\cdot A}$, where y is the $q\bar{q}$ -separation. Transforming such phase into the momentum space and applying it to the wavefunction, the second contribution $F_{\pi\gamma}^{(NV)}(Q^2)$ at $\mathbf{q}_\perp \rightarrow 0$ can be written as [4]

$$F_{\pi\gamma}^{(NV)}(Q^2)|_{\mathbf{q}_\perp \rightarrow 0} = \frac{-2}{\sqrt{3}Q^2} \int [dx] \int \frac{d^2\mathbf{k}_\perp}{16\pi^3} \left\{ \frac{(\mathbf{k}_\perp \times \mathbf{q}_\perp)^2}{(x'\mathbf{q}_\perp + \mathbf{k}_\perp)^2} \left[\frac{\partial}{\partial k_\perp^2} \Psi(x, \mathbf{k}_\perp) \right] + (x \leftrightarrow x') \right\}, \quad (8)$$

where $[dx] = dx dx' \delta(1 - x - x')$. Eq.(8) gives the expression for $F_{\pi\gamma}^{(NV)}(Q^2)$ at $Q^2 \rightarrow 0$. Here

different from Ref.[4], all the \mathbf{q}_\perp -terms that are necessary to obtain its first derivative over Q^2 are retained in our calculation and the relation $(\epsilon_\perp \times \mathbf{q}_\perp)(\mathbf{k}_\perp \times \mathbf{q}_\perp) = Q^2(\epsilon_\perp \cdot \mathbf{k}_\perp)$ is implicitly adopted. After doing the integration over \mathbf{k}_\perp , one can easily find that

$$F_{\pi\gamma}^{(NV)}(0) = F_{\pi\gamma}^{(V)}(0) = \frac{1}{8\sqrt{3}\pi^2} \int dx \Psi(x, \mathbf{0}_\perp), \quad F_{\pi\gamma}(0) = F_{\pi\gamma}^{(V)}(0) + F_{\pi\gamma}^{(NV)}(0), \quad (9)$$

which means that the valence-quark contribution $F_{\pi\gamma}^{(V)}(0)$ only gives a half to $F_{\pi\gamma}(0)$, and one can get the correct rate of the process $\pi^0 \rightarrow \gamma\gamma$ provided that the two basic contributions $F_{\pi\gamma}^{(V)}(0)$ and $F_{\pi\gamma}^{(NV)}(0)$ are considered simultaneously. Furthermore, by taking into account the PCAC prediction [17], $F_{\pi\gamma}(0) = 1/(4\pi^2 f_\pi^2)$, one can obtain the important constrain for the pion wavefunction, i.e.

$$\int_0^1 dx \Psi(x, \mathbf{k}_\perp = 0) = \sqrt{3}/f_\pi. \quad (10)$$

Without loss of generality, we can assume that the pionic wavefunction $\Psi(x, \mathbf{k}_\perp)$ depending on \mathbf{k}_\perp through k_\perp^2 only, i.e. $\Psi(x, \mathbf{k}_\perp) = \Psi(x, k_\perp^2)$ ². The expressions for $F_{\pi\gamma}^{(V)}(Q^2)$ (Eq.(2)) can be simplified after doing the integration over the azimuth angle as [9]

$$F_{\pi\gamma}^{(V)}(Q^2) = \frac{1}{4\sqrt{3}\pi^2} \int_0^1 \frac{dx}{xQ^2} \int_0^{x^2Q^2} \Psi(x, k_\perp^2) dk_\perp^2. \quad (11)$$

Similarly, the first derivative of $F_{\pi\gamma}^{(NV)}(Q^2)$ over Q^2 can be derived from Eq.(8), i.e.

$$F_{\pi\gamma}^{(NV)'}(Q^2)|_{Q^2 \rightarrow 0} = \frac{1}{8\sqrt{3}\pi^2} \left[\frac{\partial}{\partial Q^2} \int_0^1 \int_0^{x^2Q^2} \left(\frac{\Psi(x, k_\perp^2)}{x^2Q^2} \right) dx dk_\perp^2 \right]_{Q^2 \rightarrow 0}. \quad (12)$$

Furthermore, according to the definition, the pion DA at the factorization scale μ can be simplified as

$$\phi(x, \mu) = \frac{2\sqrt{3}}{f_\pi} \int_{k_\perp^2 \leq \mu^2} \frac{d^2 \mathbf{k}_\perp}{16\pi^3} \Psi(x, \mathbf{k}_\perp) = \frac{\sqrt{3}}{4\pi^2 f_\pi} \int_0^\mu \psi(x, k_\perp^2) k_\perp dk_\perp, \quad (13)$$

where the integration over the azimuth angle has been done. With the help of Eq.(13), $F_{\pi\gamma}^{(V)}(Q^2)$ can be rewritten as

$$F_{\pi\gamma}^{(V)}(Q^2) = \frac{2f_\pi}{3Q^2} \int_0^1 \frac{dx}{x} \phi(x, xQ). \quad (14)$$

Note that Eq.(14) is different from Eq.(1) only by replacing $\phi(x, \mu_0)$ to $\phi(x, xQ)$. It means that the leading contribution to $F_{\pi\gamma}(Q^2)$ as shown in Eq.(2), which was given by keeping

² The spin-space Wigner rotation might change this property for the higher helicity components as shown in Ref.[18]. Since the higher helicity components' contribution are highly suppressed for the present case, we do not take this point into consideration in the present paper.

the k_\perp -corrections in both the hard-scattering amplitude and the pion wavefunction, can be equivalently obtained by setting the upper limit for the integral of the pion DA to $\mu = xQ$. The x -dependent upper limit $[xQ]$ affects the small to intermediate Q^2 -behavior of $F_{\pi\gamma}^{(V)}(Q^2)$, and such effect will be more explicit for a wider pion DA, such as the CZ (Chernyak-Zhitnitsky)-like model [3] that emphasizes the end-point region in a strong way, as has been discussed in Ref.[5]. In literature, the pion DA is usually expanded in Gegenbauer polynomial expansion as

$$\phi(x, \mu) = \phi_{as}(x) \cdot \left[1 + \sum_{n=1}^{\infty} a_{2n}(\mu) C_{2n}^{3/2}(\xi) \right], \quad (15)$$

where $\xi = (2x-1)$, $C_n^{3/2}(\xi)$ are Gegenbauer polynomials and $a_{2n}(\mu)$, the so called Gegenbauer moments, are hadronic parameters that depend on the factorization scale μ . The Gegenbauer moments $a_{2n}(\mu)$ can be related to $a_{2n}(\mu_0)$ with the help of QCD evolution, where $\mu_0 \sim 1\text{GeV}$ is some typical hadronic energy. And to leading logarithmic accuracy, we have [10, 19]

$$a_{2n}(\mu) = a_{2n}(\mu_0) \left(\frac{\alpha_s(\mu^2)}{\alpha_s(\mu_0^2)} \right)^{\gamma_0^{(2n)}/(2\beta_0)}, \quad (16)$$

where $\beta_0 = 11 - 2n_f/3$, $\alpha_s(Q^2) = 4\pi/[\beta_0 \ln(Q^2/\Lambda_{QCD}^2)]$ and the one-loop anomalous dimension is

$$\gamma_0^{(2n)} = 8C_F \left(\psi(2n+2) + \gamma_E - \frac{3}{4} - \frac{1}{(2n+1)(2n+2)} \right). \quad (17)$$

We have to calculate $\phi(x, xQ)$ and $F_{\pi\gamma}^{(NV)}(Q^2)$ to get the whole behavior of $F_{\pi\gamma}(Q^2)$, i.e.

$$F_{\pi\gamma}(Q^2) = F_{\pi\gamma}^{(V)}(Q^2) + F_{\pi\gamma}^{(NV)}(Q^2), \quad (18)$$

where $F_{\pi\gamma}^{(V)}(Q^2)$ is determined by $\phi(x, xQ)$. The $\phi(x, xQ)$ depends on the behavior of the wavefunction $\Psi(x, \mathbf{k}_\perp)$ with the transverse-momentum dependence and its Gegenbauer moments can not be directly obtained from the QCD evolution equation (16), since $[xQ]$ can be very small and then the Landau ghost singularity in the running coupling α_s can not be avoided. As for $F_{\pi\gamma}^{(NV)}(Q^2)$, Eq.(8) presents an exact expression only at $Q^2 \sim 0$ region, and it can not be directly extended to the whole Q^2 region. The second type of contribution $F_{\pi\gamma}^{(NV)}(Q^2)$ is of higher-twist corrections associated with the $\bar{q}G \cdots Gq$ operators, which decreases as $1/Q^4$ or faster. Ref.[9] did a try to understand the high Q^2 behavior of $F_{\pi\gamma}(Q^2)$ within the QCD sum rule approach, i.e. they raised a simple picture: the sum over soft $\bar{q}G \cdots Gq$ Fock-components is dual to $q\bar{q}$ -states generated by the local axial vector current.

Furthermore, they raised an ‘effective’ pion wavefunction that includes all the Fock-states’ contributions based on the QCD sum rule analysis and then calculated $F_{\pi\gamma}(Q^2)$ within the pQCD approach. Here we will not adopt such ‘effective’ pion wavefunction to do the calculation, since we plan to extract some precise information for the valence-quark state by comparing with the CLEO experimental data.

In order to construct an expression to $F_{\pi\gamma}^{(NV)}(Q^2)$ in the whole Q^2 region, we require the following conditions at least:

- i) $F_{\pi\gamma}^{(NV)}(Q^2)|_{Q^2=0}$ should be given by Eq.(8).
- ii) $F_{\pi\gamma}^{(NV)'}(Q^2)|_{Q^2\rightarrow 0} = \partial F_{\pi\gamma}^{(NV)}(Q^2)/\partial Q^2|_{Q^2\rightarrow 0}$ should also be derived from Eq.(8).
- iii) $\frac{F_{\pi\gamma}^{(NV)}(Q^2)}{F_{\pi\gamma}^{(V)}(Q^2)} \rightarrow 0$, as $Q^2 \rightarrow \infty$.

One can construct a phenomenological model for $F_{\pi\gamma}^{(NV)}(Q^2)$ that satisfies the above three requirements to the whole Q^2 region. It is natural to assume the following form

$$F_{\pi\gamma}^{(NV)}(Q^2) = \frac{\alpha}{(1 + Q^2/\kappa^2)^2}, \quad (19)$$

where κ and α are two parameters that can be determined by the above conditions (i,ii), i.e.

$$\alpha = \frac{1}{2} F_{\pi\gamma}(0) = \frac{1}{8\pi^2 f_\pi^2} \quad (20)$$

and

$$\kappa = \sqrt{-\frac{F_{\pi\gamma}(0)}{\frac{\partial}{\partial Q^2} F_{\pi\gamma}^{(NV)}(Q^2)|_{Q^2\rightarrow 0}}}. \quad (21)$$

As for the phenomenological formula (19), it is easy to find that $F_{\pi\gamma}^{(NV)}(Q^2)$ will be suppressed by $1/Q^2$ to $F_{\pi\gamma}^{(V)}(Q^2)$ in the limit $Q^2 \rightarrow \infty$. Such a $1/Q^2$ -suppression is reasonable, since the phenomenological expression (19) can be regarded as a summed up effect of all the high twist structures of pion wavefunction, even though each higher twist structure is suppressed by at least $1/Q^4$.

III. CALCULATED RESULTS WITH THE MODEL WAVEFUNCTION

The CLEO collaboration has measured the $\gamma\gamma^* \rightarrow \pi^0$ form factor [20]. In this experiment, one of the photons is nearly on-shell and the other one is highly off-shell, with a virtuality in the range 1.5 GeV² - 9.2 GeV² [20]. There also exist older results obtained by the CELLO collaboration [21]. By comparing the theoretical prediction with the experimental results, it provides us a chance to determine a precise form for the leading Fock-state pion

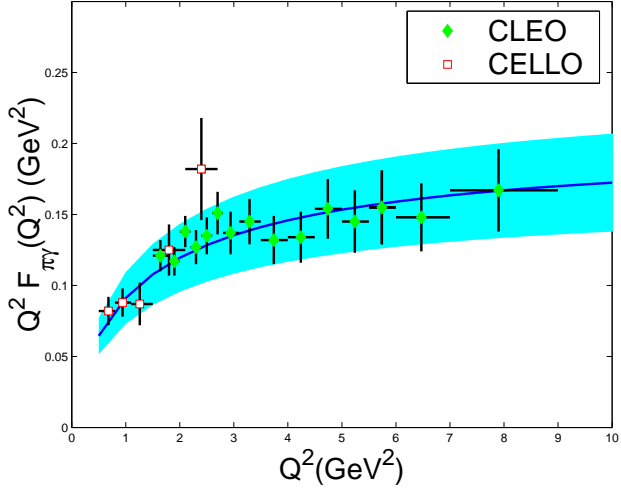


FIG. 2: The fitting curve (the solid line) for $Q^2 F_{\pi\gamma}(Q^2)$ from the CLEO and CELLO experimental data [20, 21], where a shaded band shows its uncertainty of $\pm 20\%$.

wavefunction. Similar try to determine the pion DA has been done in Refs.[22, 23] under the QCD sum rule analysis. In Fig.2, we show the fitting curve for $Q^2 F_{\pi\gamma}(Q^2)$ (derived by using the conventional χ^2 -fitting method described in Ref.[24] with slight change to make the curve more smooth) from the CLEO and CELLO experimental data, i.e. $Q^2 F_{\pi\gamma}(Q^2) \simeq 8.81 \times 10^{-7}(Q^2)^5 - 4.78 \times 10^{-5}(Q^2)^4 + 9.96 \times 10^{-4}(Q^2)^3 - 1.01 \times 10^{-2}(Q^2)^2 + 5.29 \times 10^{-2}(Q^2) + 4.48 \times 10^{-2}$ for $Q^2 \in (0.5, 10.0) \text{ GeV}^2$, where a shaded band shows its $\pm 20\%$ uncertainty ³. In fact, most of the results given in the literature, e.g. Refs. [5, 6, 7, 8, 9, 10, 11, 22], are mainly within such region. The shaded band (region) for $Q^2 F_{\pi\gamma}(Q^2)$ can be regarded as a constraint to determine the pion wavefunction, i.e. the values of the parameters in the pion wavefunction should make $Q^2 F_{\pi\gamma}(Q^2)$ within the region of the shaded band as shown in Fig.(2).

Now we are in position to calculate the pion-photon transition form factor with the help of Eq.(18). As has been discussed in the last section, we need to know the leading-twist pion wavefunction so as to derive $\phi(x, xQ)$ that is necessary for $F_{\pi\gamma}^{(V)}(Q^2)$ and to derive the values of α and κ for $F_{\pi\gamma}^{(NV)}(Q^2)$. Several non-perturbative approaches have been developed to provide the theoretical predictions for the hadronic wavefunction. One useful way is to use the approximate bound state solution of a hadron in terms of the quark model as the starting

³ It is so chosen since the sum of the statistical and systematic errors of the experimental data is $\lesssim \pm 20\%$ [20, 21].

point for modelling the hadronic valence wavefunction. The Brodsky-Huang-Lepage (BHL) prescription [4] for the hadronic wavefunction is obtained in this way by connecting the equal-time wavefunction in the rest frame and the wavefunction in the infinite momentum frame. In the present paper, we shall adopt the revised LC quark model as suggested in Ref.[18] to do our calculation, which is constructed based on the BHL-prescription and takes the following form:

$$\Psi(x, \mathbf{k}_\perp) = \varphi_{\text{BHL}}(x, \mathbf{k}_\perp) \chi^K(x, \mathbf{k}_\perp) = A \exp \left[-\frac{\mathbf{k}_\perp^2 + m^2}{8\beta^2 x(1-x)} \right] \chi^K(x, \mathbf{k}_\perp), \quad (22)$$

with the normalization constant A , the harmonic scale β and the quark mass m to be determined. The spin-space wavefunction $\chi^K(x, \mathbf{k}_\perp, \lambda)$ comes from the spin-space Wigner rotation, whose explicit expression can be found in Ref.[18]. By taking the BHL-like wavefunction (22), $F_{\pi\gamma}^{(V)}(Q^2)$ (Eq.(11)) can be simplified as

$$F_{\pi\gamma}^{(V)}(Q^2) = \int_0^1 dx \left\{ \frac{Am\beta}{\sqrt{6}\pi^{3/2}Q^2} \sqrt{\frac{x'}{x}} \left(\text{Erf} \left[\frac{\sqrt{m^2 + x^2 Q^2}}{2\beta\sqrt{2xx'}} \right] - \text{Erf} \left[\frac{\sqrt{m^2}}{2\beta\sqrt{2xx'}} \right] \right) \right\}, \quad (23)$$

where the error function $\text{Erf}(x)$ is defined as $\text{Erf}(x) = \frac{2}{\sqrt{\pi}} \int_0^x e^{-t^2} dt$. And similarly, for the limiting behaviors of $F_{\pi\gamma}^{(NV)}(Q^2)$ that are necessary to determine the parameters α and κ , we obtain

$$F_{\pi\gamma}^{(NV)}(Q^2)|_{Q^2 \rightarrow 0} = \frac{A}{8\sqrt{3}\pi^2} \int_0^1 \exp \left[-\frac{m^2}{8\beta^2 xx'} \right] dx, \quad (24)$$

$$F_{\pi\gamma}^{(NV)'}(Q^2)|_{Q^2 \rightarrow 0} = \frac{-A}{128\sqrt{3}m^2\pi^2\beta^2} \int_0^1 \frac{x}{x'} (m^2 + 4xx'\beta^2) \exp \left[-\frac{m^2}{8\beta^2 xx'} \right] dx. \quad (25)$$

The possible range for the parameters of the pion wavefunction (22) can be derived by comparing our result of $Q^2 F_{\pi\gamma}(Q^2)$ as defined in Eqs.(18,19,23) with the experiment data. Further more, the model wavefunction should satisfy the following two conventional constraints:

- The pion wavefunction satisfies the normalization [4, 18]:

$$\int_0^1 dx \int \frac{d^2 \mathbf{k}_\perp}{16\pi^3} \Psi(x, \mathbf{k}_\perp) = \int_0^1 dx \int \frac{d^2 \mathbf{k}_\perp}{16\pi^3} \frac{m}{\sqrt{m^2 + \mathbf{k}_\perp^2}} \varphi_{\text{BHL}}(x, \mathbf{k}_\perp) = f_\pi/(2\sqrt{3}). \quad (26)$$

Substituting the pion wavefunction (22) into Eq.(26), we obtain

$$\int_0^1 \frac{Am\beta\sqrt{x(1-x)}}{4\sqrt{2}\pi^{3/2}} \left(1 - \text{Erf} \left[\sqrt{\frac{m^2}{8\beta^2 x(1-x)}} \right] \right) dx = \frac{f_\pi}{2\sqrt{3}}. \quad (27)$$

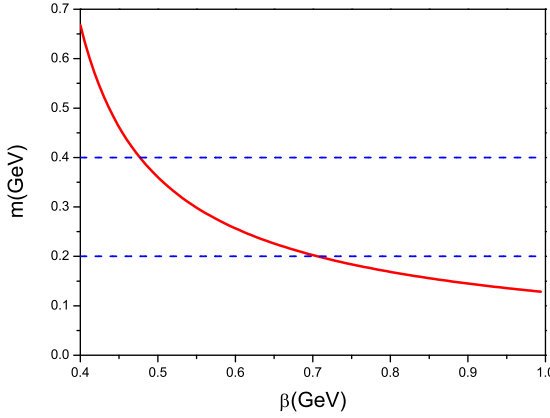


FIG. 3: The curve for the value of m versus β , which shows that for the value of m in the reasonable region of $(0.20GeV, 0.40GeV)$, $\beta \in (0.48GeV, 0.70GeV)$.

- Another constraint, as shown in Eq.(10), for the pion wavefunction can be derived from $\pi^0 \rightarrow \gamma\gamma$ decay amplitude [4], which can be further simplified with the help of Eq.(22) as

$$\int_0^1 A \exp \left[-\frac{m^2}{8\beta^2 x(1-x)} \right] dx = \frac{\sqrt{3}}{f_\pi}. \quad (28)$$

Solving Eqs.(27,28) numerically, we obtain an approximate relation for m and β , i.e.

$$6.00 \frac{m\beta}{f_\pi^2} \cong 1.12 \left(\frac{m}{\beta} + 1.31 \right) \left(\frac{m}{\beta} + 5.47 \times 10^1 \right), \quad (29)$$

which shows that the value of m is decreased with the increment of β . Fig.(3) is the curve for the value of m versus β , which shows that to restrict the value of m in the reasonable region of $(0.20GeV, 0.40GeV)$, β should be within the region of $(0.48GeV, 0.70GeV)$.

Before doing the numerical calculation for $F_{\pi\gamma}(Q^2)$, we note that Brodsky and Lepage have proposed a naive interpolation formula for both perturbative and non-perturbative regions [1], i.e.

$$F_{\pi\gamma}^{BL}(Q^2) = \frac{\sqrt{2}}{4\pi^2 f_\pi (1 + Q^2/s_0)} \left(1 - \frac{5}{3} \frac{\alpha_s(Q^2)}{\pi} \right), \quad s_0 = 8\pi^2 f_\pi^2 = 0.67GeV^2 \sim m_\rho^2 \quad (30)$$

where, as suggested in Ref.[9, 25], we have added the next-to-leading order (NLO) perturbative contribution $\left(-\frac{5}{3} \frac{\alpha_s(Q^2)}{\pi} \right)$ to the original result, which is derived without taking into account the transverse momentum into both the hard-scattering amplitude and the wavefunction, cf. Refs.[9, 10].

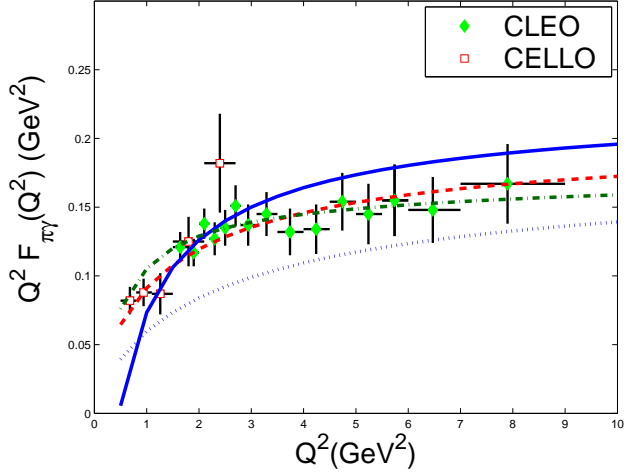


FIG. 4: $Q^2 F_{\pi\gamma}(Q^2)$ with the model wavefunction (22) for the case of $m = 0.30\text{GeV}$ ($\beta = 0.55\text{GeV}$), which is shown by a dash-dot line. The dashed line is best fit for the CLEO experimental data [20, 21], the solid line is from the interpolation formula (30) and the dotted line is the results for $Q^2 F_{\pi\gamma}^{(V)}(Q^2)$ only as $m = 0.30\text{GeV}$.

The conventional value of for the constitute quark mass m of pion is around 0.30GeV . In the present section, we concentrate our attention on the case of $m = 0.30\text{GeV}$ and we will study the uncertainty caused by varying m with a wider region of $(0.20\text{GeV}, 0.40\text{GeV})$ in the next section. We show the pion-photon transition form factor $Q^2 F_{\pi\gamma}(Q^2)$ with the model wavefunction (22) for the case of $m = 0.30\text{GeV}$ in Fig.(4), where the values for $\beta = 0.55\text{GeV}$ and $A = 25.4\text{GeV}^{-1}$ can be obtained by using the Eqs.(26,29). There we do not include the NLO contribution into our formula, since when taking into account the effects caused by the transverse-momentum dependence in the hard-scattering amplitude and the wavefunction and by the Sudakov factor, such contribution shall be suppressed to a certain degree (a naive discussion for this point has been shown in Refs.[9, 11]). Fig.(4) shows that by taking the model wavefunction (22) with $m = 0.30\text{GeV}$, the predicted value of $Q^2 F_{\pi\gamma}(Q^2)$ agrees well with the experimental data. We show the valence-quark contribution $Q^2 F_{\pi\gamma}^{(V)}(Q^2)$ in Fig.(4), which is drawn in a dotted line and its value is lower than the experimental data especially in low Q^2 region. Even though the spin-space Wigner rotation has not been adopted for the BHL-like pion wavefunction in Ref.[5], the present result for the valence-quark contribution $Q^2 F_{\pi\gamma}^{(V)}(Q^2)$ is only slightly different from that of Ref.[5] due to the fact that the contributions from the higher helicity components of pion wavefunction

are highly suppressed. As a comparison, we also draw the curve for the interpolation formula (30) in Fig.(4). It shows that $Q^2 F_{\pi\gamma}^{BL}(Q^2)$ agree with the data for small Q^2 region and it increase fast with the increment of Q^2 . Such a behavior of $Q^2 F_{\pi\gamma}^{BL}(Q^2)$ can be explained as: 1) the effective value of s_0 in $F_{\pi\gamma}^{BL}(Q^2)$ is determined by the known behavior of $Q^2 \rightarrow 0$, so $Q^2 F_{\pi\gamma}^{BL}(Q^2)$ behaves well in small Q^2 region; 2) even though $Q^2 F_{\pi\gamma}^{BL}(Q^2)$ has the right asymptotic behavior as $Q^2 \rightarrow \infty$, it does not show explicit suppression in intermediate Q^2 region for high Fock-states' contributions and those contributions might be inadequately enhanced, and then $Q^2 F_{\pi\gamma}^{BL}(Q^2)$ shows a fast rise in high Q^2 region.

IV. DISCUSSION AND COMMENT

A. Information of the valence-quark state

As shown in Fig.(4), $F_{\pi\gamma}(Q^2)$ agrees well with the experimental data by taking the leading Fock-state pion wavefunction (22) with $m = 0.30\text{GeV}$. We also show the valence-quark contribution $Q^2 F_{\pi\gamma}^{(V)}(Q^2)$ in Fig.(4), which is lower than the experimental data in low Q^2 region. This shows that one should take the non-valence quark states into account in small to intermediate Q^2 region. In fact, it has been found that the valence-quark state contribution $F_{\pi\gamma}^{(V)}(Q^2)$ fail to reproduce the $Q^2 = 0$ value corresponding to the axial anomaly [5, 7], i.e. it gives only a half of what is needed to get the correct $\pi^0 \rightarrow \gamma\gamma$ rate [17]. And to make a compensation, in Ref.[6], the valence-quark state's contribution $F_{\pi\gamma}^{(V)}(Q^2)$ has to be inadequately enhanced by replacing the leading Fock-state wavefunction to an ‘effective’ valence wavefunction that is normalized to one, e.g., the wavefunction parameters are determined by taking the charged mean-square-radius of the lowest valence-quark state of π^+ directly to the measured value for π^+ , i.e. $\langle r_{\pi^+}^2 \rangle^{q\bar{q}} = \langle r^2 \rangle_{exp}^{\pi^+}$. By taking the ‘effective’ pion wavefunction with the asymptotic-like DAs, the authors found an agreement with the experimental data for $F_{\pi\gamma}(Q^2)$ [6]. However, such an ‘effective’ pion wavefunction is no longer the leading Fock-state wavefunction itself and the probability of finding the valence Fock-state in the pion should be less than one.

By substituting the pion wavefunction (22) into the pion electromagnetic form factor, one can obtain some useful information, such as the probability of finding the valence-quark state in pion $P_{q\bar{q}}$, the mean square transverse-momentum of the valence-quark state $\langle \mathbf{k}_\perp^2 \rangle_{q\bar{q}}$

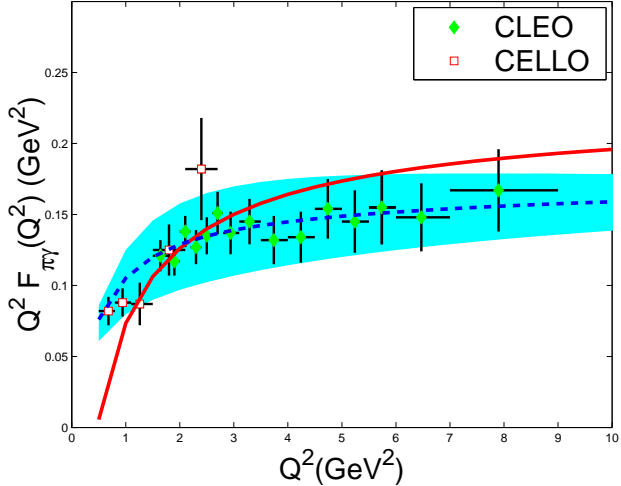


FIG. 5: $Q^2 F_{\pi\gamma}(Q^2)$ with the phenomenological model (19) for $F_{\pi\gamma}^{(NV)}(Q^2)$, with the upper edge of the band for $m = 0.40\text{GeV}$ and the lower edge of the band for $m = 0.20\text{GeV}$. The dashed line is the best fit of $Q^2 F_{\pi\gamma}(Q^2)$ for wavefunction (22) with $m = 0.30\text{GeV}$. As a comparison, the interpolation formula (30) is shown by a solid line.

and the charged mean-square-radius $\langle r_{\pi^+}^2 \rangle^{q\bar{q}}$. In Refs.[26, 27], the authors have done such a calculation within the LC pQCD approach. By adopting the formulae derived in Ref.[26] (Eqs.(24,25,27) there), one may obtain:

$$P_{q\bar{q}} = 56\%, \quad \langle \mathbf{k}_\perp^2 \rangle_{q\bar{q}} = (0.502\text{GeV})^2, \quad \langle r_{\pi^+}^2 \rangle^{q\bar{q}} = (0.33\text{fm})^2, \quad (31)$$

where we have taken $m = 0.30\text{GeV}$. All the values in Eq.(31) are summed results for all the helicity states $\lambda_1 + \lambda_2 = (0, \pm 1)$ of the valence-quark state. Eq.(31) shows that the value of $\langle r_{\pi^+}^2 \rangle^{q\bar{q}}$ is smaller than the value of the pion charged radius $\langle r^2 \rangle_{\text{expt}}^{\pi^+} = (0.671 \pm 0.008\text{fm})^2$ [28], but it is close to the value as suggested in Refs.[26, 29]. Such small $\langle r_{\pi^+}^2 \rangle^{q\bar{q}}$ for the leading Fock-state wavefunction is reasonable, since the probability of valence-quark state $P_{q\bar{q}}$ is only 56%, which confirms the necessity of taking the higher Fock-states into consideration to give full estimation of the pion electromagnetic form factor/pion-photon transition form factor, especially for lower Q^2 regions.

B. Moments of the DA from the CLEO data

In this subsection, we take a wider region for m , i.e. $m = 0.30^{+0.10}_{-0.10}\text{GeV}$, to study the Gegenbauer moments of pion DA. Under such region for m , we show the value of $Q^2 F_{\pi\gamma}(Q^2)$

in Fig.(5). The value of $Q^2 F_{\pi\gamma}(Q^2)$ will increase with the increment of m and the uncertainty caused by varying m within the region of $(0.20GeV, 0.40GeV)$ is about $\pm 20\%$. By comparing Fig.(5) with Fig.(2), it can be found that $m \in (0.20GeV, 0.40GeV)$ is a reasonable region for $Q^2 F_{\pi\gamma}(Q^2)$, which is in agreement with the experimental data in the whole Q^2 region.

From Eq.(22), we can derive the leading Fock-state pion DA that is in the usual helicity $(\lambda_1 + \lambda_2 = 0)$, i.e.

$$\phi(x, \mu_0) = \frac{Am\beta\sqrt{3}\sqrt{x(1-x)}}{2\sqrt{2}f_\pi\pi^{3/2}} \left(1 - \text{Erf} \left[\sqrt{\frac{m^2}{8\beta^2x(1-x)}} \right] \right), \quad (32)$$

where the fixed low energy scale $\mu_0 \sim 1GeV$ is explicitly written and $\phi(x, \mu_0)$ satisfies the normalization $\int_0^1 \phi(x, \mu_0) dx = 1$. By expanding Eq.(32) in the Gegenbauer polynomials as shown in Eq.(15), for $m \in (0.20GeV, 0.40GeV)$, we obtain

$$\begin{aligned} a_2(\mu_0) &= 0.002_{-0.054}^{+0.063}, \quad a_4(\mu_0) = -0.022_{-0.012}^{+0.026}, \\ a_6(\mu_0) &= -0.014_{-0.000}^{+0.009}, \quad a_8(\mu_0) = -0.006_{-0.001}^{+0.003}, \quad \dots, \end{aligned} \quad (33)$$

where the center value is for $m \simeq 0.30GeV$ that best fits the CLEO experimental data, i.e. it has the minimum χ^2 -value, and the ellipsis stands for higher Gegenbauer moments and the factorization scale μ is taken to be $\mu_0 \sim 1GeV$. For the values of $a_{2n}(\mu)$ in other factorization scales, they can be derived by QCD evolution e.g. Eq.(16). Eq.(33) shows: A) the leading-twist pion wavefunction (22) is asymptotic-like, since a_{2n} ($n \geq 1$) are much smaller than $a_0 \equiv 1$. More explicitly, the first inverse moment of the pion DA at energy scale μ_0 , $\int_0^1 dx \phi(x, \mu_0) / x = 3(1 + a_2 + a_4 + a_6 + a_8) \in (2.71, 3.20)$, which is near the same value as for the asymptotic wavefunction with $a_{2n} = 0$ ($n \geq 1$). Such a conclusion for pion wavefunction agrees with that of Ref.[30] and also agrees with a recent study that is based on the nonlocal chiral-quark model from the instanton vacuum [31]. B) a_2, a_4 will increase with the decrement of m , and $a_2 \geq 0$ if $m \leq 0.30GeV$. C) the absolute values of a_4, a_6 and a_8 are comparable to a_2 for bigger m (e.g. $m \sim 0.30GeV$); but they are suppressed to a_2 about one order for smaller m . The value of the Gegenbauer moments have been studied in various processes, cf. Refs.[31, 32, 33, 34, 35, 36]⁴. These references favor a positive value for $a_2(1GeV)$ and the most recent one is done by Ref.[33], which shows that

⁴ The present lattice results [36] disfavor the asymptotic DA, however as argued in Ref.[37], the accuracy of the lattice results needs to be further improved.

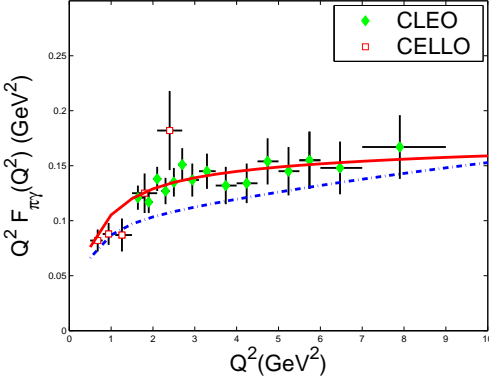


FIG. 6: Comparison of $Q^2 F_{\pi\gamma}(Q^2)$ that is derived from two different types of wavefunctions, i.e. the BHL-like wavefunction (the solid line) and the CZ-like wavefunction (the dash-dot line), under the case of $m = 0.30\text{GeV}$.

$a_2(1\text{GeV}) = 0.19 \pm 0.19$ and $a_4(1\text{GeV}) \geq -0.07$ by analyzing the leptonic mass spectrum of $B \rightarrow \pi l\nu$. Here, the range of m should be reduced to $m \in (0.20\text{GeV}, 0.30\text{GeV})$ if we require $a_2(1\text{GeV}) \geq 0$ for the pion DA.

C. Comparison with the broad wavefunction

One typical broad wavefunction is described by the CZ-like wavefunction, which can not be excluded by the pion-photon transition form factor [5] although it is disfavored by the pion structure function at $x \rightarrow 1$ [18].

We take the CZ-like wavefunction as

$$\Psi^{CZ}(x, \mathbf{k}_\perp) = A(1 - 2x)^2 \exp\left[-\frac{\mathbf{k}_\perp^2 + m^2}{8\beta^2 x(1-x)}\right] \chi^K(x, \mathbf{k}_\perp), \quad (34)$$

where an extra factor $(1 - 2x)^2$ is introduced into the pion wavefunction (22) [3]. Following a similar procedure, we find that the relation between m and β changes to

$$6.00 \frac{m\beta}{f_\pi^2} \cong 1.24 \left(\frac{m}{\beta} + 2.12\right) \left(\frac{m}{\beta} + 4.58 \times 10^1\right). \quad (35)$$

Similarly, for $m = 0.30\text{GeV}$, we have

$$P_{q\bar{q}} = 73\%, \quad \langle \mathbf{k}_\perp^2 \rangle_{q\bar{q}} = (0.496\text{GeV})^2, \quad \langle r_{\pi^+}^2 \rangle^{q\bar{q}} = (0.45\text{fm})^2, \quad (36)$$

where all the values are summed results for all the helicity states $\lambda_1 + \lambda_2 = (0, \pm 1)$ of the valence-quark state. One may observe that the second Gegenbauer moment a_2 is always

dominant over other higher Gegenbauer moments for the CZ-like DA. And for the first inverse moment of the CZ-like pion DA at energy scale μ_0 , we obtain $\int_0^1 dx \phi^{CZ}(x, \mu_0)/x = 4.69$.

In Fig.(6), we make a comparison of $Q^2 F_{\pi\gamma}(Q^2)$ that is derived from two different types of wavefunctions, i.e. the BHL-like wavefunction and the CZ-like wavefunction, under the same value of $m = 0.30 GeV$. Both the BHL-like wavefunction and the CZ-like wavefunction will lead to $Q^2 F_{\pi\gamma}(Q^2)$ within the possible region of the experimental data as shown in Fig.(2). However, the value of $Q^2 F_{\pi\gamma}(Q^2)$ derived from the BHL-like wavefunction is better than that of the CZ-like wavefunction. One may observe that the value of $Q^2 F_{\pi\gamma}(Q^2)$ caused by the CZ-like wavefunction shall increase with the increment of m , so the CZ-like model can give a better result for $Q^2 F_{\pi\gamma}(Q^2)$ in comparison to the experimental data by taking a bigger value for m , e.g. $m = 0.40 GeV$.

As a summary, we list the main differences for the BHL-like wavefunction and the CZ-like wavefunction in the following:

- By comparing with the experimental data for $Q^2 F_{\pi\gamma}(Q^2)$, one may observe that $m = 0.30^{+0.10}_{-0.10} GeV$ is a reasonable region for the BHL-like wavefunction, where the best fit to the experimental data is achieved when $m \approx 0.30 GeV$; while for the case of the CZ-like wavefunction, such region is shifted to a higher one, i.e. $m = 0.40^{+0.10}_{-0.10} GeV$, and the best fit to the experimental data is achieved as $m \approx 0.40 GeV$, which is somewhat bigger than the conventional value for the constitute quark mass of pion.
- The difference among the Gegenbauer moments e.g. $a_2(\mu_0 \sim 1 GeV)$ are big due to the different behavior of the two models. Under the condition of $m = 0.30 GeV$, the two Gegenbauer moments $a_2(\mu_0) = 0.002$ and $a_4(\mu_0) = -0.022$ for the BHL-like model (19); while for the CZ-like model (34), $a_2(\mu_0) = 0.678$ and $a_4(\mu_0) = -0.024$.
- The first inverse moments are different. Under the condition of $m = 0.30 GeV$, for the case of the BHL-like model (19), $\int_0^1 dx \phi^{BHL}(x, \mu_0)/x = 2.88$, which is close to that of the asymptotic DA; while for the case of the CZ-like model (34), $\int_0^1 dx \phi^{CZ}(x, \mu_0)/x = 4.69$, which is close to that of the original CZ-model [3].

In Ref.[37], it is shown that by taking the asymptotic DA and considering the suppression from the NLO contribution, the value of $Q^2 F_{\pi\gamma}(Q^2)$ at $Q^2 = 8.0 GeV^2$ is somewhat smaller than the experimental value $(16.7 \pm 2.5 \pm 0.4) \cdot 10^{-2} GeV^2$, i.e. $Q^2 F_{\pi\gamma}(Q^2)|_{Q^2=8.0 GeV^2} \simeq 0.115$.

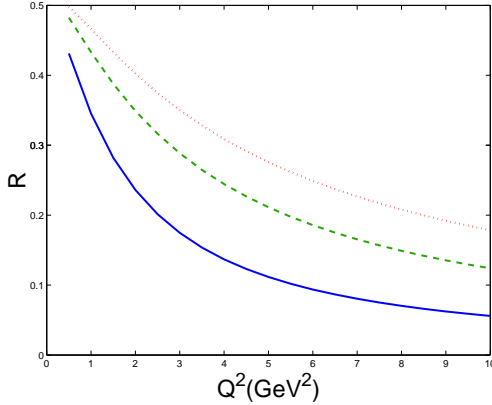


FIG. 7: The value of $R = \frac{F_{\pi\gamma}^{(NV)}(Q^2)}{F_{\pi\gamma}^{(V)}(Q^2) + F_{\pi\gamma}^{(NV)}(Q^2)}$ versus Q^2 for the BHL-like wavefunction, whose value increases with the increment of m . The dotted, dashed and solid lines are for $m = 0.40\text{GeV}$, $m = 0.30\text{GeV}$ and $m = 0.20\text{GeV}$, respectively.

However it should be pointed out that Ref.[37] is only a simple analysis, since the contribution from the k_T -dependence in both the pion wavefunction and the hard scattering amplitude, and also the contribution from $F_{\pi\gamma}^{(NV)}(Q^2)$ have not been taking into consideration. As shown in Fig.(7), even though $F_{\pi\gamma}^{(NV)}(Q^2)$ is suppressed to $F_{\pi\gamma}^{(V)}(Q^2)$ in high Q^2 region, it will have sizable contribution (about 5% – 20% at $Q^2 = 8.0\text{GeV}^2$) in the intermediate Q^2 region, e.g. it is 12% for the case of $m = 0.30\text{GeV}$.

V. SUMMARY

In this paper, we have given a comprehensive analysis on the pion-photon transition form factor $F_{\pi\gamma}(Q^2)$ involving the transverse momentum corrections with the present CLEO experimental data. As is well-known, the valence-quark state contribution dominates the pion-photon transition from factor $F_{\pi\gamma}(Q^2)$ for large Q^2 region and it makes a half of the contribution to $F_{\pi\gamma}(0)$ as one extends it to $Q^2 = 0$. One should consider the higher Fock-states contribution to $F_{\pi\gamma}(0)$ at the present experimental Q^2 region. We have constructed a phenomenological expression to estimate the contributions beyond the valence-quark state based on the exact calculation of $F_{\pi\gamma}^{(NV)}(Q^2)$ at $Q^2 = 0$. The calculated results favor the asymptotic-like behavior by comparing the different model of the pion wavefunction with the experimental data in the whole Q^2 region.

On the other hand, the present CLEO data provides the important information on the

pion DA as one has a complete expression for the pion-photon transition form factor relates two photons with one pion. Our expression for $F_{\pi\gamma}(Q^2)$ only involves the single pion DA. Thus, comparing calculated results of $F_{\pi\gamma}(Q^2)$ by taking the BHL-like pion wavefunction with the CLEO data one can extract some useful information on the pionic twist-2 distribution amplitude. Our analysis shows that (1) the probability of finding the valence-quark state in the pion is less than one, i.e. $P_{q\bar{q}} = 56\%$ and $\langle r_{\pi^+}^2 \rangle^{q\bar{q}} = (0.33 fm)^2$ with $m = 0.30 GeV$. This means that the valence Fock state is more compact in the pion and it is necessary to take the higher Fock-states into account to give full estimation of the pion-photon transition form factor and other exclusive processes. (2) under the region of $m \in (0.20 GeV, 0.40 GeV)$, we have the DA moments, $a_2(\mu_0) = 0.002^{+0.063}_{-0.054}$, $a_4(\mu_0) = -0.022^{+0.026}_{-0.012}$ and all of higher moments. Such result is helpful to understand other exclusive processes involving the pion.

ACKNOWLEDGEMENTS

This work was supported in part by the Natural Science Foundation of China (NSFC). X.-G. Wu thanks the support from the China Postdoctoral Science Foundation.

- [1] G.P. Lepage and S.J. Brodsky, Phys.Rev. **D22**, 2157(1980); *ibid.* **24**, 1808(1981).
- [2] Particle Data Group, E.J. Weinberg, *et al.*, Phys.Rev. **D66**, 010001(2002).
- [3] V.L. Chernyak and A.R. Zhitnitsky, Nucl.Phys. **B201**, 492(1982).
- [4] S.J. Brodsky, T. Huang and G.P. Lepage, in *Particles and Fields-2*, Proceedings of the Banff Summer Institute, Banff, Alberta, 1981, edited by A.Z. Capri and A.N. Kamal (Plenum, New York, 1983), P143; G.P. Lepage, S.J. Brodsky, T. Huang, and P.B. Mackenzie, *ibid.*, p83; T. Huang, in *Proceedings of XXth International Conference on High Energy Physics*, Madison, Wisconsin, 1980, edited by L. Durand and L.G. Pondrom, AIP Conf.Proc.No. 69 (AIP, New York, 1981), p1000.
- [5] Fu-Guang Cao, Tao Huang and Bo-Qiang Ma, Phys.Rev. **D53**, 6582(1996).
- [6] Bo-Wen Xiao and Bo-Qiang Ma, Phys.Rev. **D68**, 034020(2003).
- [7] R. Jakob *et al.*, J.Phys. **G22**, 45(1996); P. Kroll and M. Raulfs, Phys.Lett. **B387**, 848(1996).
- [8] A.V. Radyushkin and R. Ruskov, Nucl.Phys. **B481**, 625(1996).

- [9] I.V. Musatov and A.V. Radyushkin, Phys.Rev. **D56**, 2713(1997).
- [10] B. Melic, B. Nizic and K. Passek, Phys.Rev. **D65**, 053020(2002); F. Del Aguila and M.K. Chase, Nucl.Phys. **B193**, 517(1981); E. Braaten, Phys.Rev. **D28**, 524(1983).
- [11] N.G. Stefanis, W. Schroers and H.-Ch. Kim, Eur.Phys.J. **C18**, 137(2000).
- [12] S. Ong, Phys.Rev. **D52**, 3111(1995).
- [13] Tao Huang and Qi-Xing Shen, *Proceedings of the international seminar of Quark'90*, Telavi, USSR, (1990), Ed. by Matveev *et al.*, page 340; Z.Phys. **C50**, 139(1991).
- [14] J. Boots and G. Sterman, Nucl.Phys. **B325**, 62(1989); H.N. Li and G. Sterman, Nucl.Phys. **B381**, 129(1992).
- [15] G.P. Lepage, S.J. Brodsky, T. Huang and P.B. Mackenzie, in *Particles and Fields-2*, page 83, Invited talk presented at the Banff summer Institute on Particle Physics, Banff, Alberta, Canada, 1981.
- [16] S.J. Brodsky, H.C. Pauli and S.S. Pinsky, Phys.Rept. **301**, 299(1998); and references therein.
- [17] S. Treiman, R. Jackiw and D. Gross, *Lectures on the Current Algebra and its Applications*, Princeton University Press (Princeton, 1972).
- [18] T. Huang, B.Q. Ma and Q.X. Shen, Phys.Rev. **D49**, 1490(1994).
- [19] Dieter Mueller, Phys.Rev. **D51**, 3855(1995).
- [20] CLEO collaboration, V. Savinov *et al.*, hep-ex/9707028; CLEO Collaboration, J. Gronberg *et al.*, Phys.Rev. **D57**, 33(1998).
- [21] CELLO collaboration, H.-J. Behrend *et al*, Z.Phys. **C49**, 401(1991).
- [22] A. Schmedding and O. Yakovlev, Phys.Rev. **D62**, 116002(2000).
- [23] A.P. bakulev, S.V. Mikhailov and N.G. Stefanis, Phys.Lett. **B508**, 279(2001).
- [24] W.H. Press, S.A. Teukolsky, W.T. Vetterling and B.P. Flannery, *Numerical Recipes in Fortran 77: The Art of Scientific Computing, Second Editon*, Published by the Press Syndicate of the University of Cambridge (1992), p650.
- [25] S.J. Brodsky, C.R. Ji, A. Pang and D.G. Robertson, Phys.Rev. **D57**, 245(1998).
- [26] Tao Huang, Xing-Gang Wu and Xing-Hua Wu, Phys.Rev. **D70**, 053007(2004); Xing-Gang Wu and Tao Huang, Int.J.Mod.Phys. **A21**, 901(2006).
- [27] F. Cardarelli, *etal.*, Phys.Rev. **D53**, 6682(1996).
- [28] S.R. Amendolia, *etal.*, Phys.Lett. **B146**, 116(1985).
- [29] B. Povh and J. Hufner, Phys.Lett. **B245**, 653(1990); T. Huang, Nucl.Phys. (Proc. Suppl.) **7**,

320(1989).

- [30] P. Kroll and M. Raulfs, Phys.Lett. **B387**, 848(1996); A.P. Bakulev, S.V. Mikhailov, N.G. Stefanis, Phys.Lett. **B508**, 279(2001), Erratum: *ibid* **B590**, 309(2004).
- [31] Seung-il Nam, Hyun-Chul Kim, Atsushi Hosaka and M. M. Musakhanov, hep-ph/0605259.
- [32] V.M. Braun, A. Khodjamirian and M. Maul, Phys.Rev. **D61**, 073004(2000).
- [33] P. Ball and R. Zwicky, Phys.Lett. **B625**, 225(2005).
- [34] A. Schmedding and D. Yakovlev, Phys.Rev. **D62**, 116002(2000).
- [35] A.P. Bakulev, K.P. Kumericki, W. Schroers and N.G. Stefanis Phys.Rev. **D70**, 033014(2004); Erratum-*ibid*.**D70**, 079906(2004).
- [36] L. Del Debbio, M. Di Perro and A. Dougall, Nucl.Phys.Proc.Suppl. **119**, 416(2003); M. Gockeler, hep-lat/0510089.
- [37] V.L. Chernyak, hep-ph/0605327.